JOURNAL OF MATERIALS SCIENCE **37** (2002) 5319–5325

Microstructure and martensite transformation in aged Ti-25Ni-25Cu shape memory melt spun ribbons

J. MORGIEL
Institute of Metallurgy and Materials Science, Polish Academy of Sciences, 25 Reymonta st., 30-059 Kraków, Poland
E-mail: office@imim-pan.krakow.pl

E. CESARI, J. PONS
Departament de Fisica, Universitat de lesIlles Balears, Ctra. De Valldemossa km7.5, E-07071 Palma, Spain

A. PASKO
Institute of Metal Physics, National Academy of Sciences, 36 Vernadsky Blvd., Kiev 252142, Ukraine

J. DUTKIEWICZ
Institute of Metallurgy and Materials Science, Polish Academy of Sciences, 25 Reymonta st., 30-059 Kraków, Poland

The phase transformations and microstructure of Ti-25at.%Ni-25at.%Cu alloy melt-spun at 26 m/s (50 μm thick, 3 mm wide) were investigated using DSC and TEM. The as received ribbon was nearly fully amorphous with a few spherical β phase grains (of size up to 15 μm). The heating (20°C/min.) of this ribbon resulted first in restart of growth of existing large grains and later in homogenous nucleation and growth of new small β phase crystallites within the amorphous matrix. The crystallization peak temperature of amorphous parts in this ribbon was determined to be 460°C. Further heating with the same rate to higher temperatures causes precipitation predominantly at grain boundaries with maximum of its thermal effect around 600°C. Isothermal aging of crystallized ribbon cause precipitation of thin plates of a tetragonal phase. The size and density of these plate-like precipitates depends on local microstructure and differs most drastically within large primary grains. The *in situ* TEM experiments confirmed the presence of only B2–B19 martensite transformation in the investigated ribbon. However, *in situ* TEM observations showed also that this transformation was significantly retarded in areas with small grains and even more in areas of high dislocation density as compared to primary large grains. Therefore, the delay in martensitic transformation caused by differences in the microstructure was the reason for the peak splitting in DSC curves.

1. Introduction

Alloying of Ni-Ti with more than 10 at.% Cu allows to obtain shape memory alloys (SMA) with larger recoverable strains [1] in a narrower temperature range within which this effect can be used [2]. Moreover, substitution of nickel with copper in these alloys reduces the composition sensitivity of the martensitic start temperature M_s [3], making the production of SMA within sharply specified temperature range much easier. However, excessive brittleness of alloys with high copper additions during conventional casting and thermo-mechanical processing [4] stimulated interest in other production techniques like melt spinning.

The equi-atomic TiNi alloy has high melting temperature of 1350°C and therefore is not best suited for melt spinning but additions of up to 25 at.% Cu is decreasing it to 1025°C [5]. The first experiments with melt spinning of Ni-Ti-Cu alloys confirmed that they are easy to cast and the resulting ribbons show good shape memory effect [6–11]. Thermal cycling leads to single stage B2–B19 transformation explaining the tight hysteresis observed in these ribbons. One of recent report on martensite structure in TiNiCu alloys indicated that the tetragonal structure of B19 martensite have a slight monoclinic distortion [12]. Unfortunately, some experiments in NiTiCu ribbons with higher Cu content suggested that the much sought suppression of the next

B19–B19′ martensite to martensite transformation is not always effective [9].

Limited observation of the microstructure showed that the as cast Ti-40Ni-10Cu ribbons are crystalline and characterized by relatively large grain size exceeding several microns [7]. An increase of the copper content up to 25 at.% allowed to produce ribbons of mostly amorphous matrix with few but also large circular grains of B2 phase [9, 10]. The presence of an unidentified nanocrystalline phase in such "as cast" Ti-Ni-Cu ribbons was also reported in [9]. The complex multi-component microstructure of as cast ribbons would definitely influence the subsequent shape memory effect. Therefore, a necessity of further study of the microstructure of this ribbon is clearly evident as separately suggested in [9].

The aim of the present paper was to correlate changes of the microstructure of Ti-25at.%Ni-25at.%Cu ribbons showing reversible martensitic transformation during aging at temperatures within the crystallization range.

2. Experimental procedure

The Ti-25at.%Ni-25at.%Cu alloy was cast in vacuum and homogenized at 750°C for 4 hours. Next, pieces of around 3 cm^3 were heated just above melting temperature and cast on a copper wheel rotating at 26 m/s. The resulting ribbons were around 50 μm thick and 3 mm wide.

The characteristic martensitic transformation temperatures were determined from DSC measurements performed on a Perkin–Elmer DSC 7 calorimeter with heating/cooling speed of 20°C/min. The microstructure observations were carried out with a Hitachi-H600 (100 kV) and Philips CM20 (200 kV) transmission microscopes respectively. The *in situ* heating experiments were performed using the first one equipped with Hitachi single tilt heating holder. Thin foils were prepared by standard double jet electropolishing like in [11].

3. Results

The calorimetric measurements of the homogenized bulk material showed strong single peaks both on cooling and heating cycles resulting from the martensitic transformation. The same measurements of the ribbon produced low and broad peaks with a long tail on the low temperature side (curves described "as cast" in Fig. 1). The characteristic martensitic transformation temperatures and the heat of transformation of bulk alloys and as-spun ribbons measured on these DSC curves are summarized in Table I. For parts of ribbon aged at different times in calorimeter, where several overlapping peaks are usually present, the peak position along with overall heat effect was listed in Table II.

Heating of the ribbon at 20°C/min to higher temperatures produced a strong sharp exothermic peak at 460°C, corresponding to the crystallization, and a broad one at around 600°C. Heating the ribbon with the same rate and next aging it at 450°C (Fig. 1) first shifted the small peak corresponding to martensite transformation (present already in as cast condition—marked with ✦) toward slightly higher temperatures and simultaneously stepped its higher temperature slope. Next, within the lower temperature tail a new peak started to form (marked with ★). Further aging caused formation and fast growth of a new peak (marked with ✹). Still longer aging caused shift of positions of all peaks toward higher temperatures. In the final stage, i.e., before lowering of the transformation energy (1 hour), the peaks tended to sharpen so their splitting or development of sidearm is more pronounced. The reverse martensitic transformation was affected by aging in the same way, i.e., first a small peak showed "one side sharpening" and was shifted to slightly higher temperatures. Only then a new peak started to grow. The only significant difference was that the new peak is wider in reverse than in forward transformation and because of that it overlapped any other side peaks. However, in the last stages of aging this new highest peak sharpened showing sidearm corresponding to the separate peak on the cooling curve. The aging process was stopped after one hour when the thermal effects due to martensitic transformation started to diminish.

The microstructure observations of the as cast ribbon showed that it is mostly amorphous with large—spherical in plan view—crystallites of B2 phase (Fig. 2a). These crystallites are either single or grouped in small colonies (Fig. 2b). In some cases the exposure of material to low temperatures during double jet polishing in electrolyte cooled down to −20°C starts a martensitic transformation which reverses when the thin foil is transferred to microscope results in formation of "shadow" image delineating position of former martensite plates. The above effect is caused by "irreversible" distortion caused to surface oxide layer during martensite transformation. The external boundaries of such colonies are smooth and always bowing out, while their internal boundaries usually show some corrugation.

TABLE I Characteristic temperatures and energy of martensitic transformation in bulk alloy and as cast ribbon

Material	M_s (°C)	M_f (°C)	A_s (°C)	A_f (°C)	A_p (°C)	M_p (°C)	E (J/g)
Bulk	61	45	60	75	67	55	15
Ribbon	22	−13	−1	32	19	9	∼1.5

TABLE II "Peak" temperatures of martensitic (M_{p1}, M_{p2}, Mp3) and reverse (A_{p1}, A_{p2}, A_{p3}) transformation in ribbon aged in calorimeter at 450°C

Aging time (min.)	M_{p1} (°C)	M_{p2} (°C)	M_{p3} (°C)	A_{p1} (°C)	A_{p2} (°C)	A_{p3} (°C)	Energy (J/g)
As cast[a]	–		6.8	15.9	–	–	∼1.5
0.1	–	8.0	21.2	30.0	17.5	–	2.4
1	17.4	13.0	24.0	30.0	28.3	–	3.2
3	21.0	15.8	26.3	30.0	34.0	–	11.2
5	24.1	17.8	29.6	32.0	36.6	–	11.1
10	25.7	19.6	31.3	35.0	38.4	–	11.4
20	26.5	20.4	31.8	37.8	39.7	–	11.3
40	26.8	22.0	33.1	38.5	41.4	43.0	11.2
60	26.2	21.7	34.4	38.7	41.3	45.7	10.5

[a]The same material as in Table I but in this table peak positions are presented.

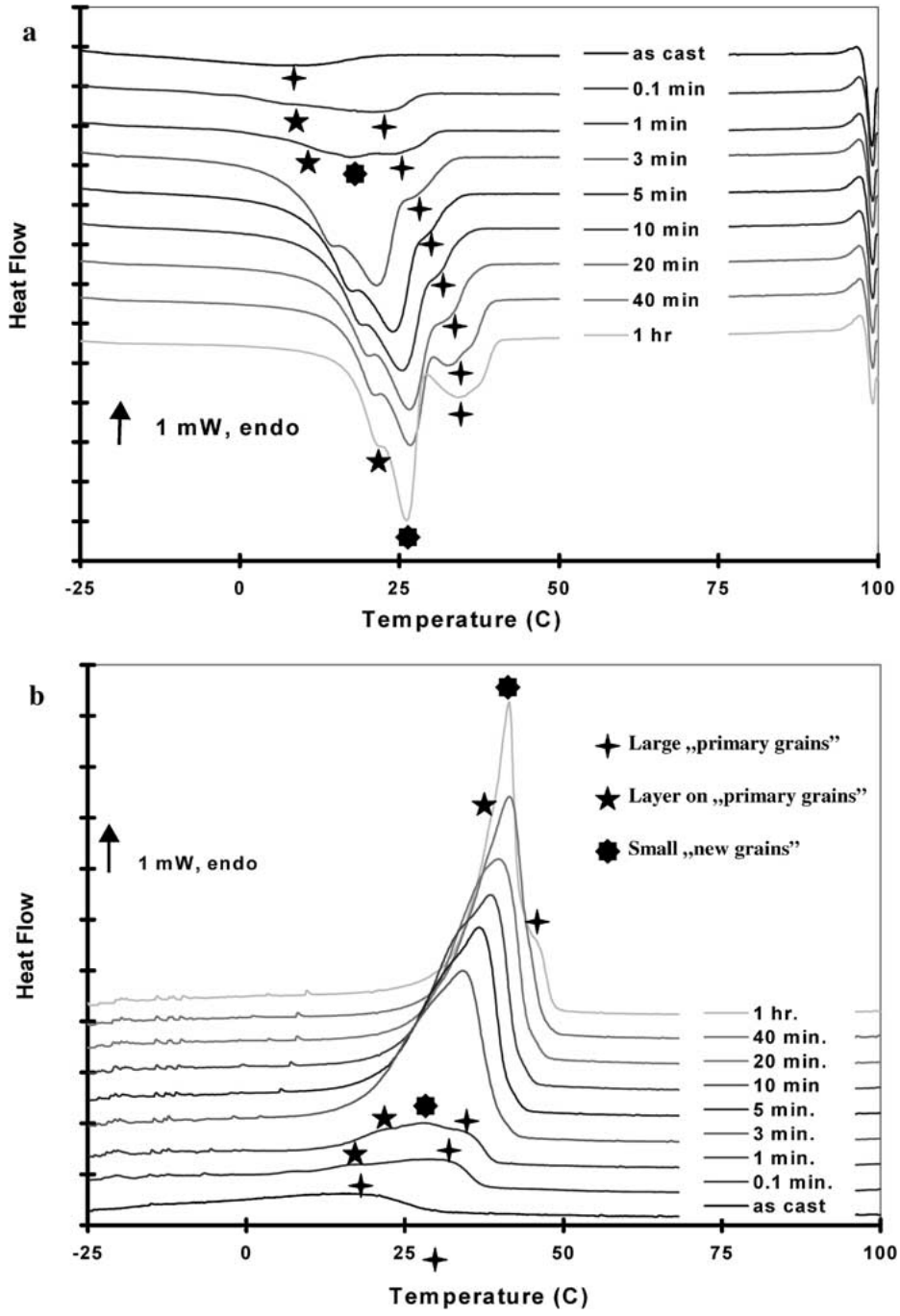

Figure 1 DSC curves of martensitic (a) and reverse (b) transformation in the ribbon aged at 450°C.

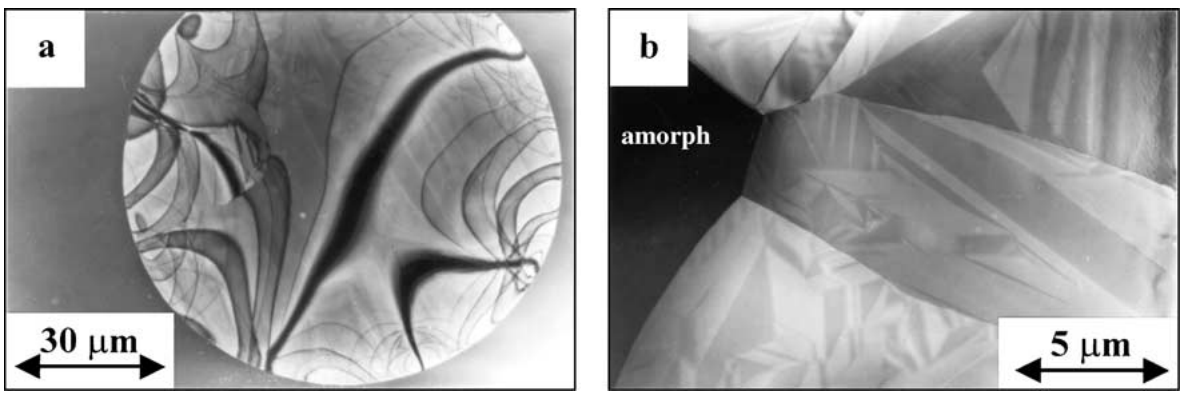

Figure 2 Microstructure of Ti-25Ni-25Cu ribbon in as spun condition: (a) large single grain surrounded by amorphous matrix, (b) crystalline grains surrounding pocket of amorphous material (marked as "amorph").

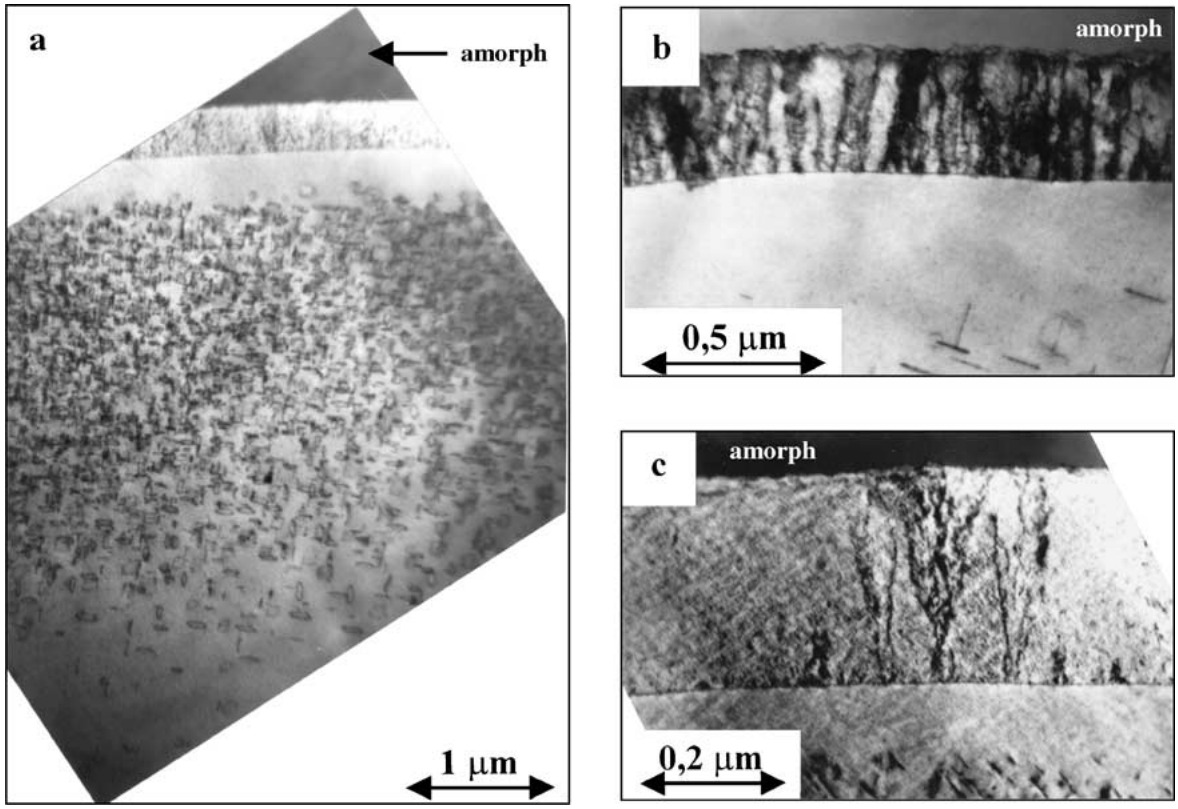

Figure 3 Microstructure of Ti-25Ni-25Cu ribbon *in situ* aged at 450°C for 2 min.; (a) general view of part of a circular grain, (b) outer part in contact with amorphous matrix, (c) thin area of the layer grown during ageing.

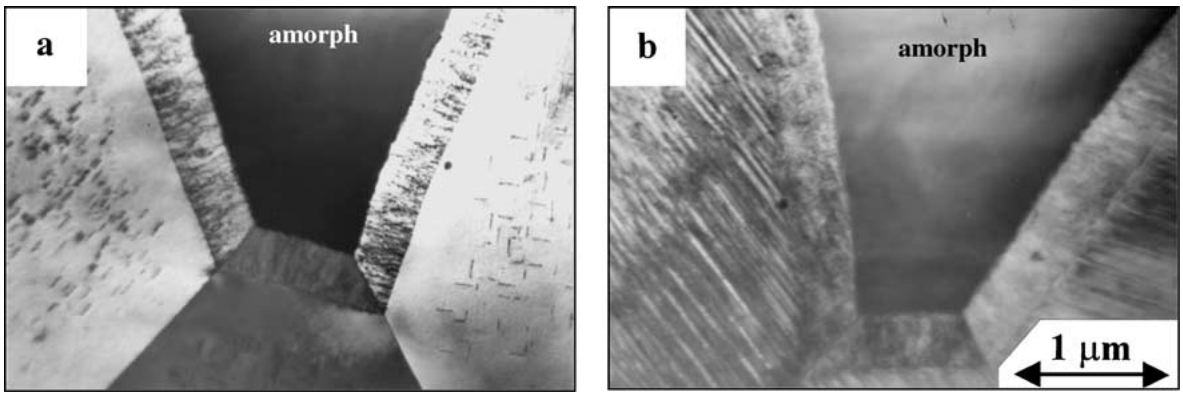

Figure 4 Ti-25Ni-25Cu ribbon *in situ* (a) aged at 450°C/2 min. and (b) cooled to R.T.

Aging at 450°C first caused nucleation of plate like phase within large grains (Fig. 3). However, both grain centers and a narrow strip adjacent to boundaries remain free of these plates. The narrow strip may be compared with classical precipitate free zone present in most aged precipitates hardenable aluminium alloys. The image darkening toward the grain center (bottom of Fig. 3a) was caused rather by increasing thickness in this place than the diffused bend contours (which in this case runs from top to bottom, but only on the right side of this figure). Therefore, the contrast from the few precipitates present there is clear enough to confirm their local density decrease in this area. The changing precipitate density is most probably a result of different vacancy concentration in the spherical grains in as cast condition. Simultaneously, at this early stage of aging, the external boundaries of already existing grains restart their growth into amorphous matrix adding a strip of similarly oriented and heavily faulted material (Fig. 4b and c). The defects are mostly dislocations running parallel to growth direction. Inside this newly grow strip the plate like precipitates are also present but they are so tiny that their presence is practically revealed only by basket wave contrast (Fig. 3c). Similar microstructure features were observed in thin foils from pieces of ribbon heat treaded in DSC (Fig. 1, curve after 1 min. of aging).

The *in situ* cooling of ribbon with such microstructure resulted first in formation of relatively long set of parallel martensite plates and only later at lower temperature much finer plates were formed in newly crystallized heavily faulted strip of material at the outskirts of large grains (Fig. 4a and b).

Longer aging at 450°C results in homogenous nucleation and fast growth of new crystallites within remaining amorphous parts of ribbon causing formation

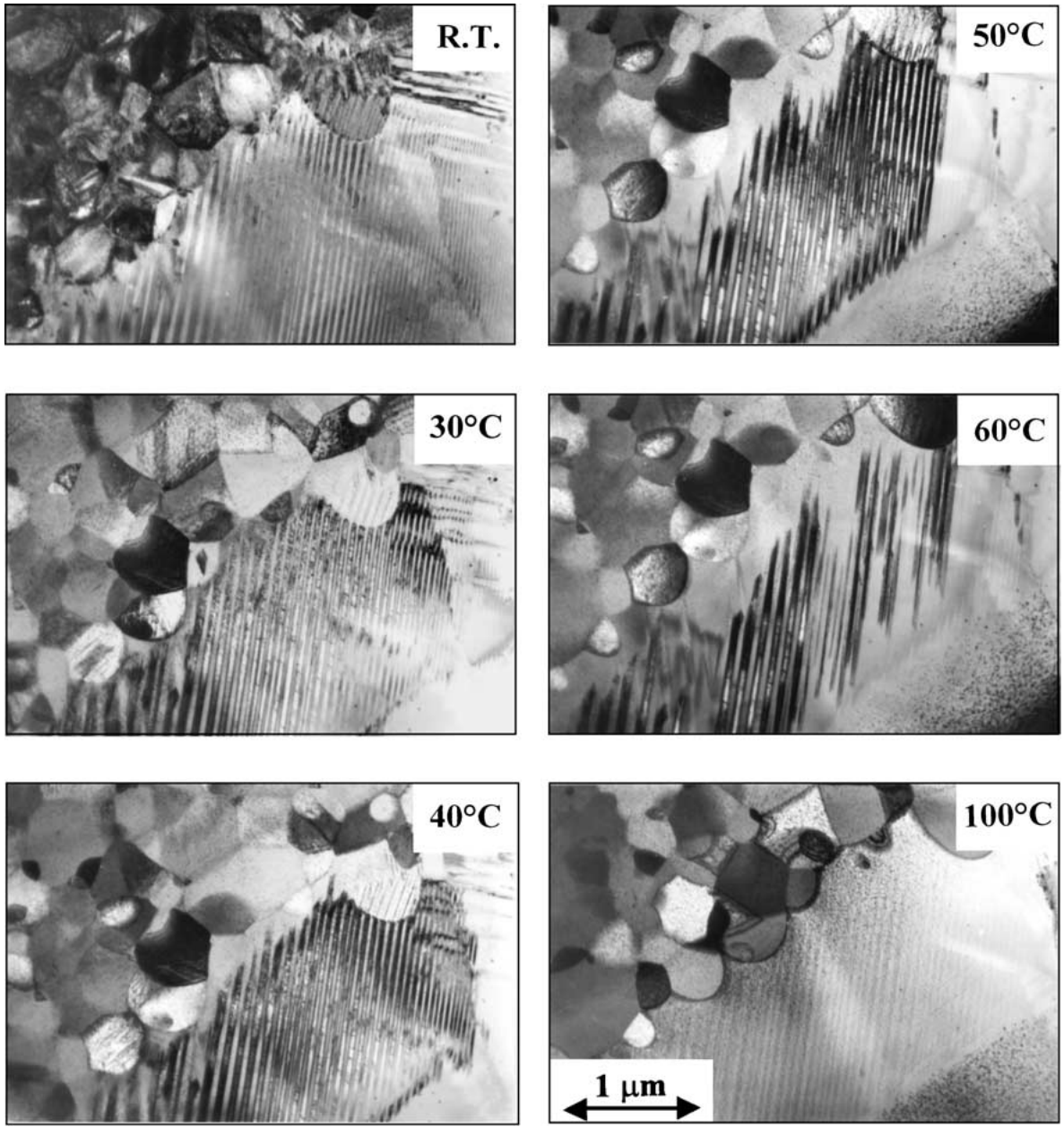

Figure 5 Ti-25Ni-25Cu ribbon *in situ* heating of the ribbon first aged at 450°C/2 min. and next cooled to R.T.

of large areas of submicron equiaxed grains (Fig. 5—100°C). Cooling of such samples to room temperature (R.T.) causes its transformation to martensite (Fig. 5—R.T.). It occurs in the following sequence: first the centers of large grains transform, next newly formed small equiaxed grains and finally transforms the most heavily faulted strip re-grown at the surface of primary circular grains. The *in situ* heating causes a reverse sequential transformation to B2 phase as shown in series of images presented in Fig. 5. Heating up from R.T. first to 30°C causes "shrinking" of all the plates from large grains centers but only a few of martensite platelets from small grains. At that stage of heating the martensite formed in most heavily faulted strips at the rims of large grains remains nearly unchanged. Rising the foil temperature up to 40°C removes the martensite plates from the small grains but still leaving the bordering strip untouched, i.e., filled with martensite plates. Only further *in situ* heating caused gradual removal of martensite plates from that strip changing it again to the β phase. The aging at higher temperatures of 550°C and 650°C, causes fast homogenous nucleation of new B2 phase grains within the amorphous material (Fig. 6a and b). The new grains fill up fast all the available space. Further aging causes growth of existing precipitates and nucleation of new ones both in the primary and in the new grains.

4. Discussion

The crystalline as cast Ti-40Ni-10Cu ribbons are characterized by grains exceeding several microns [4, 6, 7], what is a relatively coarse microstructure for melt spinning technique. The increase up to 25 at.% Cu in these alloys allows obtaining nearly fully amorphous ribbons but always with a number of large spherical crystallites of β phase, as reported previously [9, 11] and observed presently. The optical microscopy observation of this ribbon in cross section presented

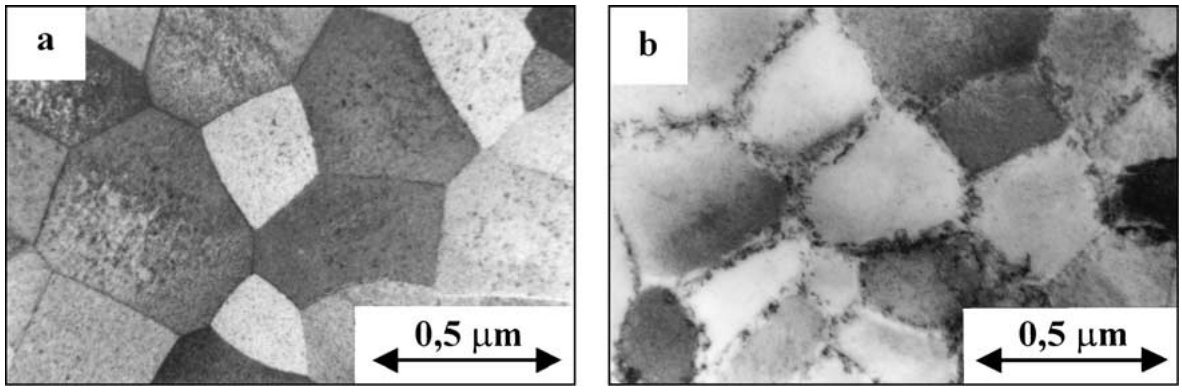

Figure 6 Ti-25Ni-25Cu ribbon *in situ* aged at (a) 550°C/5 min. and (b) 650°C/1 min.

elsewhere [13] confirmed both their spherical shape and that no surface layer was formed in other cases [14]. The presence of these few large crystallites indicates low density of nuclei and high growth rate of the β phase during melt spinning. Therefore, further increase of the wheel speed or diminishing of the nozzle opening is necessary to produce fully amorphous ribbons.

On the other hand, the *in situ* TEM heating experiments [10] proved that the nuclei density during aging between 400°C and 500°C is so high that it made practically impossible to form any grain larger than half micron. Therefore, the coarse (2–10 μm) spherical grains in ribbons of the same composition and aged at slightly lower temperature of 410°C could not be a result of crystallization as reported in [11] but formed as in other cases [9] during the melt spinning process. Therefore, the microstructure of heterogeneously nucleated columnar grains formed in contact with the wheel [11] or mixed amorphous matrix and large spherical grains [9, 10] might be eventually substituted by sub micron grains obtained during aging, provided fully amorphous ribbon is obtained first. Even as the additional heat treatment compromises the production simplicity of the melt spinning, the above approach might allow to get shape memory materials with unique microstructure promising improvement in their mechanical properties.

This unique fine grain microstructure is stabilized during aging at temperatures within the crystallization range by precipitates forming both inside and at grain boundaries as documented in this work. At higher temperatures precipitation at grain boundaries dominates. Therefore, the wide peak present above crystallization temperature cannot be connected with crystallization as suggested by Xie *et al*. [9] but with the maximum of the precipitation.

The nearly crystalline in as cast condition Ti-25Ni-25Cu ribbons show double peaks during temperature cycling within the martensite transformation range [9]. However, the electron diffraction patterns taken at temperatures lower than both peaks (i.e., at R.T.) showed solely presence of orthorhombic martensite. The above and the lack of monoclinic B19′ martensite in present observations may indicate that, also in the high copper NiTiCu ribbons there is only one stage transition from parent B2 to orthorhombic B19 martensite as proposed by Rosner [11] and excluding a two stage B2–B19–B19′ as suggested by Xia *et al*. [9]. The presence of the B19′ monoclinic martensite was confirmed in their investigation only with electron diffraction and therefore could have been caused by thin foil effects. On the other hand, the DSC peak splitting in as spun ribbon in [9, 11] could have been caused by the presence of zones of different defect density—as documented in this work—interfering with the nucleation and growth of martensite within this areas, rather than by two subsequent martensite transformation.

The side peaks formed during later stages of aging in the presently investigated ribbon have their explanation also in the formation of areas or zones drastically different both in defects and precipitates distribution. The best example is given by comparing the microstructure of large spherical grains after aging with its centers free from precipitates, next zone of precipitates followed by zone free from precipitates adjacent to grain boundary and finishing with the layer of heavily faulted material added during aging. Such precipitates are similar to the TiCu plate-like ones reported by Rösner *et al*. [12]. The sharp peaks dominating after long aging should be on the other hand connected with the new small homogeneously nucleated grains.

The first *in situ* TEM cooling showed that the martensite transformation starts first within the large primary grains, next in small equiaxed grains and finally in strip of material grown at the outside of large grains. The retarding of martensite transformation in equiaxed grains might be connected with the effect of their smaller grain size, whereas the still lower start of martensite transformation in strips grown at the sides of large grains can be explained through their high dislocations density. However, precise explanation of each thermal effect by relevant microstructure details would be possible only after further *in situ* experiments.

5. Conclusions

1. The Ti-25Ni-25Cu ribbon cast at 26 m/s is nearly fully amorphous with a small fraction of large spherical β phase grains. The crystallization peak temperature of amorphous parts in this ribbon was determined to be 460°C. Heating to higher temperatures results in increased precipitation with maximum of its thermal effect around 600°C.

2. Aging of the as cast ribbon within the range of crystallization temperature results first in both restart of

growth of large primary grains and formation of plate-like precipitates within them. Next homogenous nucleation of new grains in remaining amorphous material takes place. High nuclei density of new grains results in sub micron grain size of those parts of crystallized ribbons.

3. Aging of crystallized ribbon cause precipitation of thin plates of a tetragonal phase similar with that described by Rösner *et al*. [12]. The size and density of these plate precipitates differ drastically within large primary grains formed during melt spinning being probably one of the reasons of DSC peak splitting during martensite transformation.

4. Only the B2–B19 martensite transformation in the Ti-25Ni-25Cu ribbon has been confirmed during *in situ* TEM experiments. The martensite transformation was slightly retarded in areas of smaller grains and even more in heavily dislocated strip grown at primary crystallites as compared to large primary crystallites.

Acknowledgement

Financial support from DGI, Ministerio de Ciencia y Tecnología (project PB98–0127) is gratefully acknowledged.

References

1. T. SABURI, in Proc. ICOMAT 92, edited by C. M. Wayman and J. Perkins (Monterey Inst. of Advanced Studies, 1993) p. 857.
2. T. H. NAM, T. SABURI, Y. NAKATA and K. SHIMIZU, *Mat. Trans. JIM* **31** (1990) 1050.
3. O. MERCIER and K. N. MELTON, *Met. Trans.* **10A** (1979) 387.
4. Y. FURUYA, M. MATSUMOTO, H. KIMURA and T. MASUMOTO, *Mat. Sci. Eng.* A **147** (1991) L7.
5. T. ZHANG, A. INOUNE and T. MASUMOTO, *ibid.* **181/A182** (1994) 1423.
6. Y. FURUYA, M. MATSUMOTO, H. KIMURA, K. AOKI and T. MASUMOTO, *Mat. Trans. JIM* **31** (1990) 504.
7. Y. FURUYA, M. MATSUMOTO and T. MASUMOTO, in Proc. ICOMAT 92, edited by C. M. Wayman and J. Perkins (Monterey Inst. of Advanced Studies, 1993) p. 905.
8. M. N. MATVEEVA, V. A. LOBODJUK, V. I. KOLOMYCEV and I. D. LOVCOVA, *Metally* (1991) 164.
9. Z. L. XIE, J. VAN HUMBEECK, Y. LIU and L. DELAEY, *Scripta Materialia* **379** (1997) 363.
10. J. DUTKIEWICZ, J. MORGIEL and T. CZEPPE, in Proc. Conf. on El. Microscopy, Cancun, 1998, edited by H. A. Calderon and M. J. Yacaman, p. 29.
11. H. RÖSNER, A. V. SHELYAKOV, A. M. GLEZER, K. FEIT and P. SCHLOßMACHER, *Mat. Sci. and Eng.* A **273–275** (1999) 733.
12. H. RÖSNER, P. SCHLOßMACHER, A. V. SHELYAKOV and A. M. GLEZER, *Scripta Mat.* **43** (2000) 871.
13. L. LITYŃSKA, PH. VERMAUT, J. MORGIEL, J. DUTKIEWICZ, P. OCHIN and R. PORTIER, *J. Phys. IV France* **11** (2001) Pr8-357.
14. H. RÖSNER, A. V. SHELYAKOV, A. M. GLEZER and P. SCHLOßMACHER, *Mat. Sci. and Eng.* A **307** (2001) 188.

Received 30 April 2001
and accepted 29 March 2002